

Influence of Laser Beam Profile on Nd³⁺:YAG Laser Assisted Formation of Polycrystalline-Si Films in Underwater Conditions

Esther Blesso Vidhya Y, Sriram R and Nilesh J Vasa

Department of Engineering Design, Indian Institute of Technology, Chennai, 600036, India

E-mail: estherblessoanand@gmail.com

Influence of the Gaussian, flat-top and line beam profiles of the second harmonic pulsed Nd³⁺:YAG laser on the formation of a polycrystalline-silicon (poly-Si) on a-Si thin film in water ambience was investigated. Amorphous silicon (a-Si) thin films with thickness of 1000 nm and 400 nm deposited on crystalline Si (c-Si) substrates were treated with different laser-fluence values under water. In order to induce texturing of surface along with annealing, laser beam overlap technique with different percentages of spot overlap was used. The fluence window for crystallization was experimentally analyzed through in-situ reflectivity measurements. Surface morphology, crystalline characteristics and electrical characteristics were studied to confirm the extent of crystallization. The percentage of improvement in the crystallinity was estimated based on the suppression of the a-Si broad band in the XRD analysis. It was estimated to be 82% corresponding to the laser fluence ranging from ≈ 260 mJ/cm² to 450 mJ/cm² for 50% of spot overlap. The crystalline characteristics of the film obtained with the Gaussian, line and the flat-top beam profiles were comparable for higher percentage of overlapping. However, uniform distribution of the texture height was obtained with the flat-top and the line beam profiles. Results obtained with under-water treatment showed improvement compared to that in the air.

DOI: 10.2961/jlmn.2015.03.0018

Keywords: Polycrystalline-Si, Amorphous-Si, Laser annealing, Crystallization, Flat-top laser beam, Line Beam, Solar cells, Texturing, Thin films

1. Introduction

Solar photovoltaic technology is most promising technology to meet the increasing energy demand. Majority of solar cells use silicon as a material due to its efficiency, stability and availability but it is limited by the thickness of the material [1]. Amorphous silicon (a-Si) thin films are considered since they possess a larger band gap (1.7 eV) than crystalline silicon (1.1 eV). Hence, they absorb the visible part of the solar spectrum more effectively than the infrared portion of the spectrum and offer material saving. However efficiency is limited due to the absence of crystal structure and the presence of dangling bonds which adversely affect the mobility of a-Si resulting in low photovoltaic efficiency. Recently, poly-Si is widely used in solar photovoltaic cells due to its abundance, stability, low toxicity, and cost effectiveness. Efficiency of a-Si film can be improved by a rapid thermal annealing approach, such as laser annealing technique to produce poly silicon films [2,3].

The reduction of reflection is an essential part of achieving a high efficiency solar cell and it is also essential to absorb the light in the solar cell. The amount of light absorbed depends on the optical path length and the absorption coefficient. The reflections from the surface can be reduced by the formation of textured surface which will also increase the optical path length. This means creating a roughened surface so that the incident light may have a better probability of being absorbed in to the solar cell. crystallization of a-Si and surface texturing on a-Si thin

film can be achieved simultaneously through laser processing [4].

Most studies of laser annealing and texturing on a-Si are performed by irradiating samples in vacuum or in the presence of a gas with femtosecond laser. Here the results of nanosecond laser irradiation of a-Si films in water ambience are presented. In this work, the influence of laser beam profile and the solid-state Nd³⁺:YAG laser annealing fluence with a Gaussian, a line and a flat-top intensity distribution on a-Si crystallization was studied. Crystallization fluence window was determined using an in-situ reflectivity measurement technique. Experimental study was performed for the Gaussian, Line and flat-top laser beam with wavelength of 532 nm in water ambience. Surface texturing was achieved with different percentages of laser spot overlapping. Surface morphology analysis was performed with the atomic force microscopy (AFM). Crystallization characteristics were studied by using the scanning electron microscopic (SEM) imaging, the X-Ray diffraction analysis and the Raman spectroscopy analysis. Resistance and Photoconductivity measurements have been performed to investigate the optical and electronic properties of the laser annealed and textured samples.

2. Experimental Investigations

2.1 Laser Annealing and Texturing

The schematic of in-situ reflectivity measurement and laser annealing setup is shown in Figure 1. In-situ reflectivity measurement technique was used to investigate the

influence of laser fluence in order to determine the process window for possible crystallization without ablation [4]. The experiment was performed using a solid-state, Q-switched Nd³⁺:YAG laser (Brilliant b, Quantel) with the wavelength of 532 nm. Pulse duration of the SHG output was 6 ns and the beam profile was Gaussian. Amorphous-Si (a-Si) films with a thickness of 1 μm and 400 nm were deposited by the PECVD technique (Hindhivac) on c-Si substrate with a thickness of $\approx 270 \mu\text{m}$. During the laser annealing with the laser pulse duration of only 6 ns, it was difficult to measure the temperature rise at the irradiated spot. Therefore a different approach was adopted where in the reflectivity of the melt zone was measured using a probe laser beam (diode laser, 635 nm). Nd³⁺:YAG laser gives pump beam and 670 nm diode laser beam was used as continuous wave probe beam. The high energy pump beam intercepts the sample surface at normal incidence.

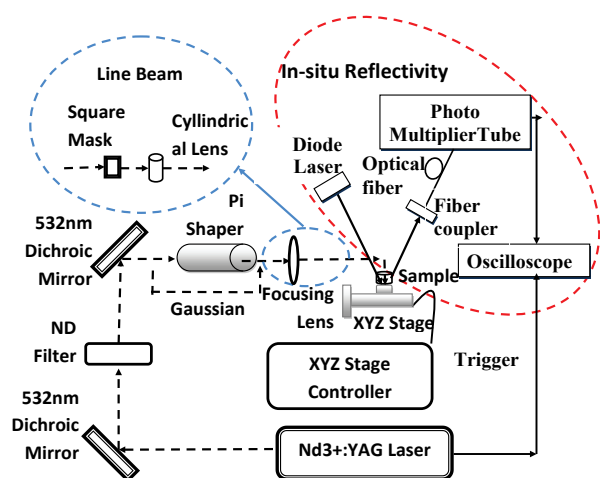


Fig. 1 Experimental setup for nanosecond Laser annealing with Flat-top, Line and Gaussian beam profiles.

Low energy probe beam was made to incident on the sample surface at an angle of 45°. The reflected probe beam was routed to the photomultiplier tube (PMT) which converts the intensity variation into voltage variation. This voltage output was captured in fast high resolution digitized oscilloscope (6100A, Lecroy). Reflectivity measurements were performed with different laser fluence values. Figure 2 shows the change in the reflectivity of the probe laser beam corresponding to different laser fluence values

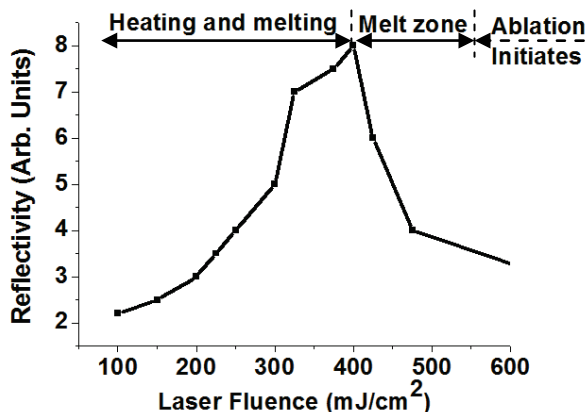


Fig. 2 Reflectivity change for different laser fluences.

used while irradiating a-Si film in air. Approximate fluence range for various zones such as heating, melting and ablation are also shown in Fig. 2. When the laser fluence value crossed the threshold, solid a-Si began to melt, and the excited carrier density increased. As the reflectivity of liquid phase a-Si is greater than that of solid phase, reflectivity of the probe beam also increased which indicates increase in the temperature during the heating and the melting stage. When the laser fluence value was increased beyond the melting regime, the temperature of the molten pool increased and the reflectivity decreased as shown in Fig. 2 similar to the works reported elsewhere [5,6]. When the laser fluence was increased further, the temperature of the molten pool increased to the boiling temperature and vaporization was initiated. As a result surface damage was observed. Fluence window up to boiling temperature was considered for annealing. These results were in good agreement with the theoretically estimated fluence window.

Laser annealing was performed with the laser beam profiles of Gaussian, Line and Flat-top. 10 mm \times 10 mm sample was scanned with the laser with different percentage of spot overlapping, such as 30 %, 50% and 90% for the Gaussian and flat-top beam profiles and 0%, 50 % and 90% for line beam in both rows and columns with a pulse repetition rate of 1 Hz. Samples were scanned by moving the sample and the laser position was fixed. A pi shaper (π Shaper 12_12_532_HP, AdlOptica) was used to change the Gaussian output from the laser into a flat-top beam profile. Flat-top beam was converted in to a line beam by using a square mask and a cylindrical lens. The samples were kept under 3 mm depth of deionized water and the laser beam was focussed to a 2 mm diameter spot by using 200 mm focal length lens for Gaussian and flat top and 2 mm width line by using 300 mm focal length cylindrical lens for line beam. To investigate the influence of the laser fluence on annealing and ablation processes, a-Si films were treated with different fluence values by altering the laser beam energy. The speed of X-Y stage movement was controlled to get the desired spot overlapping.

To investigate the surface morphology, the samples were analyzed through scanning electron microscope (SEM) (FEG, Quanta 200). To investigate the crystallinity, the films were characterized by using the Raman spectroscopy (Jusco 5000 series) and X-Ray Diffraction (Bruker, Discover D8) techniques. The texturization on the samples were analyzed though Atomic Force Microscopy (Keyence, VN-8000M/8010M). Electric resistance (using the four-probe technique) and I-V measurements of treated and untreated samples were performed using the electrical source/measurement unit (Keysight, B2901A).

3. Results and Discussions

3.1 Laser crystallization of a-Si

Figure 3 shows SEM images of ns laser annealed samples in underwater with the Gaussian (30%) and the flat-top (50%) beam profiles. A single laser pulse formed surface structures resembling ripples on a liquid surface. Microscope images show that the annealed region contains few of these ripple-like structures. When the pulses were overlapped, the surface texture with overlapping ripple structures was observed. As the percentage of overlapping was

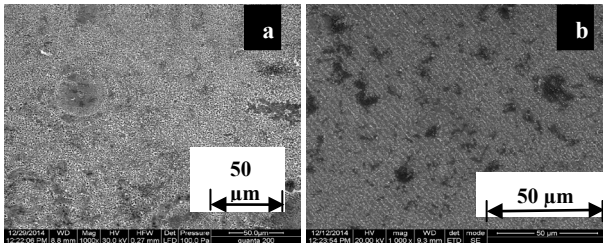


Fig. 3 SEM micrographs of a-Si/c-Si samples treated with ns-laser at 532 nm with fluence value of 450 mJ/cm² under water (a) Gaussian with 30% spot overlap (b) Flat-top with 50% spot overlap (1000X magnification).

increased the surface roughness also changed due to the interaction of many ripple structures. After 90% overlapping of laser pulses, the surface was covered with sub-micrometer size bead-like structures.

There are several possible mechanisms reported by which the bubbles may produce the wave-like structures shown in figure 3 [7]. Diffraction effect combined with the local heat convection effect may result in a capillary wave in the molten silicon through Marangoni flow [8-10]. Superposition of ripple structures caused by multiple laser pulses might have produced the randomly distributed sub micrometer beads.

Figure 4 shows SEM microphotographs of ns-laser annealed samples with varying fluences in underwater with the Gaussian and the flat-top beam profiles. Samples were scanned with 90% spot overlapping. Figure 4 (a) shows the SEM micrograph of the untreated a-Si/ c-Si where no trace of surface modification was observed. On the other hand, surface change was observed on the laser treated samples as shown in Figs. 4(b) to (d). In the a-Si/c-Si samples treated with a low laser fluence of 170 mJ/cm², a spheribead-like structure was noticed as shown in Fig. 4(c). When the laser fluence was further increased to 260 mJ/cm² and 450 mJ/cm², the size of the bead-like structure increased as shown in Fig. 4(d), which was treated as an indication of complete melting. In the case of the laser treatment with the flat-top beam profile, uniform change in surface mor-

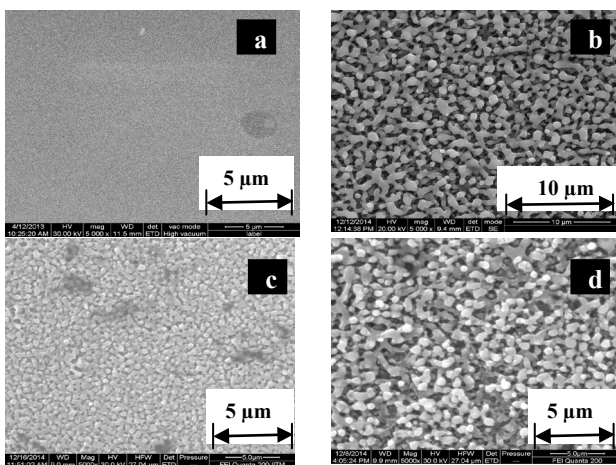


Fig. 4 SEM micrographs of a-Si/c-Si samples (a) untreated and treated with ns-laser at 532 nm with (b) fluence value 450 mJ/cm² with gaussian and different fluence values of (c) 170 mJ/cm² (d) 450 mJ/cm² with Flat-top beam profile in water ambience with 90 % spot overlapping. (5000× magnification).

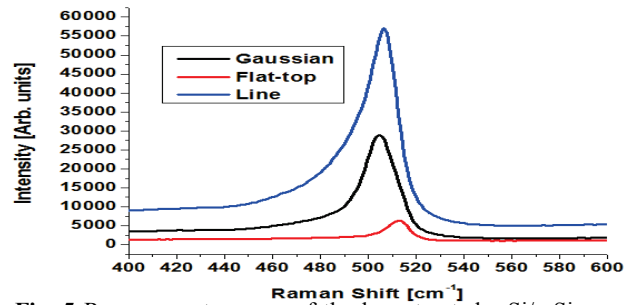


Fig. 5 Raman spectroscopy of the laser treated a-Si/c-Si samples in underwater with different beam profiles at fluence 450 mJ/cm².

phology was observed. On the other hand, in the case of the Gaussian beam profile, regions with different sizes of bead like structures were observed. Thus for uniform annealing and texturing the flat-top profile was useful.

Underwater annealing produced smaller high density structures compared to annealing in air environment. This smaller size formation in water must be due to a reduction in capillary wavelength in water ambience [11,12]. The molten silicon layer solidify much faster in water than in air, as the thermal conductivity and heat capacity of liquid water were greater than those of air. The dispersion relation for capillary waves in a shallow layer of molten silicon indicates that reduction in the lifetime of the liquid layer decreases the longest allowed capillary wavelength [12]. It has been reported that the longest allowed capillary wavelength is about 1 μm. Because the cooling time was reduced by the flow of heat to the surrounding water in the experiments presented here, the longest allowed wavelength should be less than 1 μm resulting in smaller structures [7,13,14].

To confirm the crystallization characteristics of the laser annealed a-Si, Raman spectroscopic analysis was performed. The untreated a-Si on crystalline silicon (a-Si/c-Si) sample shows a Raman spectrum with a sharp peak around 501 cm⁻¹ and a pronounced shoulder on the low frequency side, which might be associated with the convolution of the amorphous phase around 480 cm⁻¹. The peak was shifted from a typical value of around 470 cm⁻¹ corresponding to a-Si, which might be due to the effect of crystalline substrate. The effect on crystallization with different laser beam profiles such as the Gaussian, the flat-top within the region of crystallization was investigated by treating the samples at varying laser fluence and different percentage of the beam

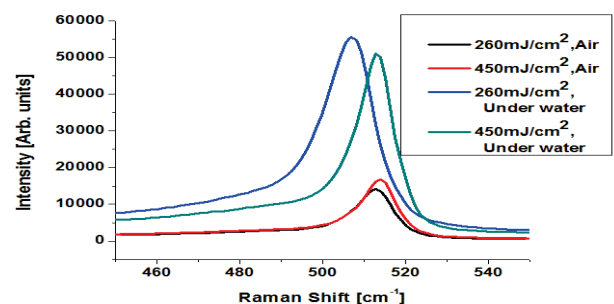


Fig. 6 Raman spectroscopy of the laser treated a-Si/c-Si samples at 532 nm underwater with different laser fluences and different ambience with gaussian with 90% spot overlapping.

overlap (Figure 5). Raman spectra of the laser treated samples with 50% overlapping with the Gaussian, the line and the flat-top shows shift in Raman peak values to 509, 511 and 514 cm^{-1} , respectively, which are very close to the crystalline peak value of around 520 cm^{-1} . As the percentage of overlapping increases, the spectral width is reduced and the peak shifts towards the c-Si spectrum. In the case of the flat-top and line beam annealing, more narrowing and shifting of the peak was observed as compared with the Gaussian which indicates uniform annealing. However with increase in the laser fluence and with 90% spot overlap, all three beam profiles show similar results.

For lower laser fluences, laser annealing in air shows better crystallization properties than that in water (Figure 6). As the fluence value increased, the laser annealing under both ambience were comparable. This might be due to the increase in the melting threshold energy under water because of some of the light absorption by water, scattering of light by the water surface and bubbles and decrease in surface temperature due to the water cooling [15].

In addition to Raman spectroscopic analysis, X-ray Diffraction (XRD) analysis was also performed so as to confirm the nature of crystallization and to determine the orientation of the grains. Figures 7(a) and (b) show XRD results of the untreated and laser treated a-Si/c-Si samples. In the case of untreated a-Si/c-Si a broad spectrum representing the amorphous nature of the silicon around $2\theta = 25^\circ$

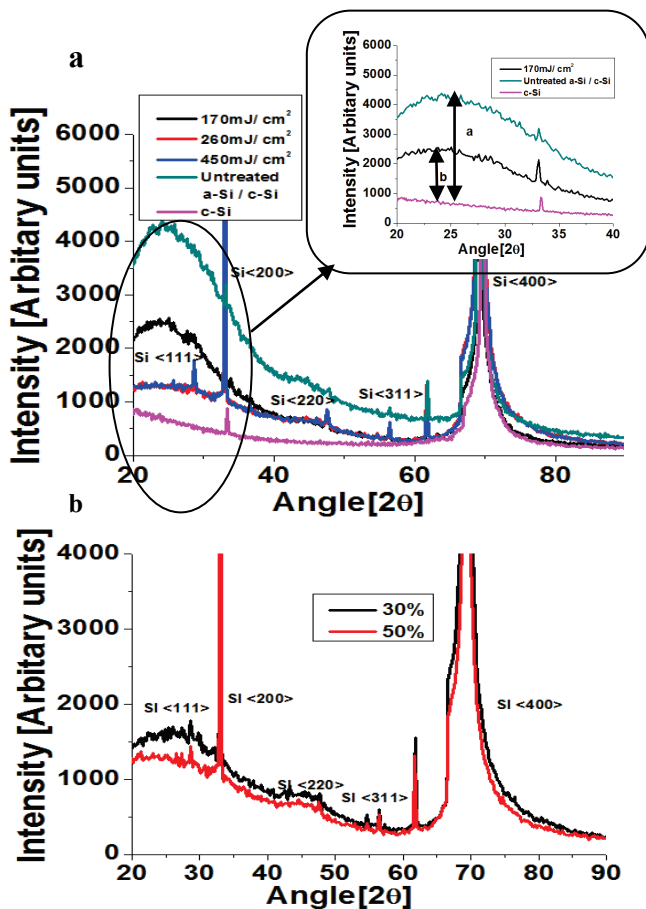


Fig. 7 XRD data of the (a) untreated and laser treated a-Si/c-Si sample for different laser fluences with 50% spot overlap and (b) different percentage of overlapping at 450mJ/cm² with Flat-top beam profile underwater.

along with XRD peak related to substrate c-Si (100) were observed. The peak at 61.7° appears due to the CuK β radiation diffracted from the Si(400) planes. The improved crystallinity in the treated samples was estimated based on the suppression of the amorphous band after laser treatment by taking XRD pattern of c-Si as reference. The percentage suppression was calculated by using a formula $\frac{a-b}{a} \times 100\%$, where a and b are intensity of untreated a-Si and laser treated samples, respectively, corresponding to the XRD pattern of c-Si at the angle of 25°.

Figure 7 shows the XRD data of the laser treated a-Si/c-Si samples at the laser wavelength of 532 nm with different laser fluence values and different percentage of overlapping with Flat-top beam profile. The main substrate peak is at 69.15°, which is the (400) peak for Si. An additional peak at ~ 33° has been observed which was due to the reflection from Si (200) planes. The (200) peak was also a forbidden reflection and it appears due to double diffraction effects. The peak at 61.7° appears due to the CuK β radiation diffracted from the Si(400) planes [16]. When the laser fluence value was increased, the broad spectrum of amorphous silicon reduces. The presence of Si peaks <111>, <220>, and <311> confirms the poly crystalline nature of the film which confirms crystallization. Based on the XRD analysis, quenching of the amorphous region was observed in the laser treated samples. The percentage of improvement in the crystallinity compared to a-Si was estimated to be ~46%, 82% and 82% for the fluence values 170 mJ/cm², 260 mJ/cm² and 450 mJ/cm², respectively. On the other hand, the percentage improvement in the crystallinity for 30% of spot overlap was estimated to be ~74% with the laser fluence of 450 mJ/cm². Based on XRD data,

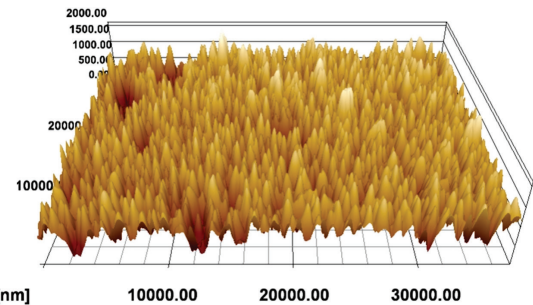


Fig. 8 AFM image of laser treated a-Si/c-Si at 90% overlap with Flat-top beam profile under water with fluence 450 mJ/cm².

more quenching of amorphous spectrum was observed in flat-top treated samples in water.

3.2 Texture Formation

Formation of Textures during annealing was observed by means of Atomic Force Microscopy. Figure 8 shows AFM image of the laser textured a-Si film samples at the 90% of beam overlap corresponding to the flat-top beam profile in water ambience. The AFM images show the formation of conical structures. The density and uniformity of conical peaks increases with the flat-top beam profile and water ambience compared to that in air.

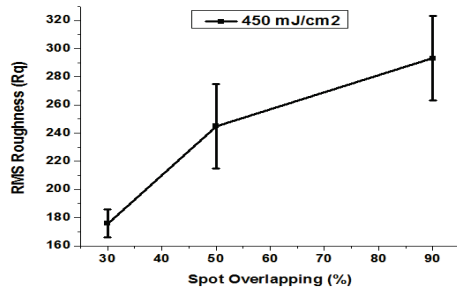


Fig. 9 Surface roughness Rq (nm) versus different percentage of spot overlapping of samples treated in water.

Root mean square (RMS) value of surface roughness (Rq parameter) was estimated based on AFM images. Figure 9 shows variation of surface roughness (Rq) values of the samples treated in underwater with different percentages of beam overlap. The increase in surface roughness was observed for the increase in laser fluence and increase in the percentage of spot overlapping in the melting region. Significant difference in the surface roughness parameter (Rq) was observed between the samples treated in air and underwater. For lower and medium fluence values, samples treated in air show higher Rq values. For higher fluence values no significant difference was observed between air and water treatment.

3.3 Electrical characterization

To investigate the effect of annealing on flow of electrons through the a-Si film, resistance measurements were performed. Four probe resistance measurements of treated and untreated samples were performed using a precision source /measurement unit (B2901A, Keysight) to confirm crystallization. The sheet resistance of an a-Si/c-Si sample without laser annealing was found to be around 900 Ω/Sq . By laser annealing, a-Si becomes crystallized, so that conductivity through the grains increases so the resistance decreases. When the samples were treated at the wavelength of 532 nm with the flat-top and the line beam in water, the resistance was found to be less compared to Gaussian for the laser fluence ranging from 170 to 450 mJ/cm^2 , as shown in Figure 10(a). The sheet resistance decreased as the overlapping percentage increased.

Photovoltaic properties, such as photoconductivity of the laser treated and nano-textured samples were investigated. The textured surface can play a significant role in improving the amount of incident light absorption through multiple-reflections. I-V characterization was performed by illuminating the laser treated sample with Xe light source with the power of 250 Watts. Current and voltage measurements were performed with the precision source / measurement unit (B2901A, Keysight).

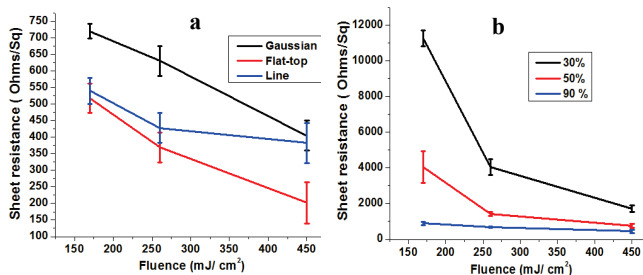


Fig. 10 Resistance of ns- laser treated samples at the wavelength of 532 nm treated with different fluences in water (a) different beam profiles with 90% overlap (b) different percentage of overlapping with flat-top.

Measurements were performed with the precision source / measurement unit (B2901A, Keysight).

Figure 11(a) and (b) shows current- voltage measurements

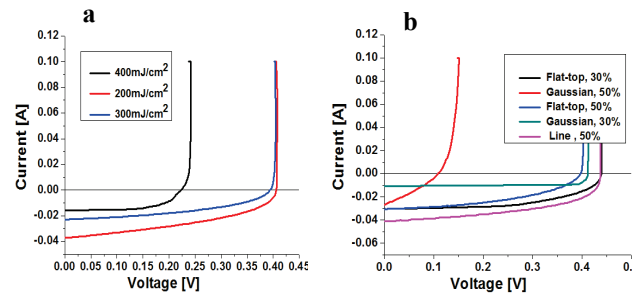


Fig. 11 I-V characteristics of samples laser treated in water with flat-top beam (a) different fluences with 90% overlap (b) different beam profiles with 400 mJ/cm^2

of laser treated samples. High V_{oc} and I_{sc} were observed for low fluence and reduces at high fluence which might be due to the ablation at high fluence with high percentage of overlapping. The ablation threshold decreases with increasing number of pulses due to modification of the absorption behavior of the film such that ablation occurs at fluence levels lower than the previous pulse. Therefore material will be removed by high energy input. The samples treated with the flat-top and the line beams showed higher value of V_{oc} and I_{sc} when compared to the samples treated with the Gaussian beam with 30% and 50% of overlapping. No significant difference was observed for higher percentage of overlapping. The results of the samples treated with low percentage of spot overlapping with high fluence were comparable with the sample treated with 90% spot overlapping with low laser fluence.

4. Conclusion

Application of nano-second pulsed, solid-state Nd^{3+} :YAG laser for annealing of a-Si films in water ambience was demonstrated. The influence of beam profile, spot overlapping and laser fluence on the annealing of amorphous silicon films was investigated experimentally. The laser fluence for efficient conversion from a-Si to polycrystalline silicon films was estimated to be between 150 and 400 mJ/cm^2 . High density and smaller sized conical spikes were observed in water annealing compared to air. Although the texture height was slightly lower in water annealing than in the air ambience, the amorphous band was suppressed more than that of the laser annealing in air. The percentage of improvement in the crystallinity was estimated based on the suppression of the broad band a-Si around 25°. It was estimated to be 82% corresponding to the laser fluence ranging from $\approx 260 \text{ mJ}/\text{cm}^2$ to 450 mJ/cm^2 for 50% of spot overlap. For low laser fluence high percentage of spot overlapping and for higher fluences low percentage overlapping was required to get the comparable results. The crystalline characteristics of the film after laser annealing with higher percentage of overlapping using the Gaussian, line and the flat-top beam profiles were comparable. Nevertheless, uniform distribution of the texture height was obtained with the flat-top and the line beam profile. Results obtained with under-water treatment showed improvement compared to that in the air.

Acknowledgments

This work was supported by Department of Science and Technology, Government of India (Project # SR/S3/MERC/0085/2010(G)). The authors are grateful to the members of Microelectronics and MEMS Laboratory, Department of Electrical Engineering, Scanning Electron Microscope and X-ray diffraction analysis Facilities in the Department of Metallurgy and Raman spectroscopy, Department of Physics of IIT Madras for providing the facilities for characterization.

References

- [1] R. B. Bergmann : Appl. Phys A., 69, (1999) 187.
- [2] A. K. Ghosh, C. Fishman, and T. Feng: J. Appl. Phys., 51, (1980) 446.
- [3] J. M. Poate : "Laser annealing of semiconductors" (Academic press, 1982) p. 40.
- [4] I. A. Palani, N. J. Vasa, and M. Singaperumal: Mat. Sci. Semicon. Proc., 11, (2008) 107.
- [5] I. Boneberg, O.Yavas, B. Mierswa, and P. Leiderer: Phys. Status Solidi B., 174, (1992) 295.
- [6] S. Theppakuttai, D. B. Shao, and S.C. Chen: J. Manuf. Processes., 6, (2004) 24.
- [7] M. Y. Shen, C. H. Crouch, J. E. Carey, and E. Mazur: Appl. Phys. Lett., 85,(2004) 5694.
- [8] A. Ben-Yakar, R. L. Byer, A. Harkin, J. Ashmore, H. A. Stone, M. Shen, and E. Mazur: Appl. Phys. Lett., 83, (2003) 3030.
- [9] E. N. Glezer, C. B. Schaffer, N. Nishimura, and E. Mazur: Opt. Lett., 22, (1997) 1817.
- [10] C. B. Schaffer, N. Nishimura, E. N. Glezer, A. M.- T. Kim, and E. Mazur: Opt. Express., 10, (2002) 196.
- [11] S. I. Dolgaev, S. V. Lavrishev, A. A. Lyalin, A. V. Simakin, V. V. Voronov, and G. A. Shafëev: Appl. Phys. A: Mater. Sci. Process., 73, (2001) 177.
- [12] M. Y. Shen, C. H. Crouch, J. E. Carey, R. Younkin, E. Mazur, M. Sheehy and C. M. Friend: Appl. Phys. Lett., 82, (2003) 1715.
- [13] S. D.Ferris, H. J. Leamy, and J. M. Poate: AIP Conf. Proc.,(ed by American Institute of Physics, New York, 1979), p. 1.
- [14] D. K. Fork, G. B. Anderson, J. B. Boyce, R. I. Johnson, and P. Mei: Appl. Phys. Lett., 68, (1996) 2138.
- [15] K. L.Choo, Y. Ogawa, G. Kanbargi, V. Otrá, L. M. Raff, and R.Komanduri: Material Science and Engg., 372, (2004) 145.
- [16] A. Gupta, D. Paramanik, Varma, and C. Jacob: Bulletin of Materials Science, 27-5, (2004) 445.

(Received: May 26, 2015, Accepted: December 17, 2015)